

## RAPID COMMUNICATION

# Engineering dislocation-rich plastic zones in ceramics via room-temperature scratching

Xufei Fang<sup>1</sup>  | Oliver Preuß<sup>1</sup> | Patrick Breckner<sup>1</sup> | Jiawen Zhang<sup>2</sup> | Wenjun Lu<sup>2</sup>

<sup>1</sup>Department of Materials and Earth Sciences, Technical University of Darmstadt, Darmstadt, Germany

<sup>2</sup>Department of Mechanical and Energy Engineering, Southern University of Science and Technology, Shenzhen, P. R. China

**Correspondence**

Xufei Fang, Department of Materials and Earth Sciences, Technical University of Darmstadt, 64287 Darmstadt, Germany. Email: [fang@ceramics.tu-darmstadt.de](mailto:fang@ceramics.tu-darmstadt.de)

**Funding information**

Deutsche Forschungsgemeinschaft, Grant/Award Number: 414179371

**Abstract**

In this communication, we demonstrate a simple but powerful method to engineer dislocations into large plastic zones in various single-crystal ceramic materials via room-temperature scratching. By using a Brinell indenter with a diameter of 2.5 mm, we successfully produced plastic zones with a width and depth of  $\sim 150$   $\mu\text{m}$  in a single scratch track, while the length of the scratch track can be arbitrarily long depending on the sample size. Increasing the number of repetitive scratching cycles increases the dislocation density up to  $\sim 10^{13}$   $\text{m}^{-2}$  without visible crack formation. The outlined experimental procedure is showcased on single-crystal  $\text{SrTiO}_3$ ,  $\text{MgO}$ ,  $\text{ZnS}$ , and  $\text{CaF}_2$  to demonstrate the general applicability of this technique. In light of the increasing research interest in dislocation-tuned functional and mechanical properties in ceramics, our method will serve as a simple, fast, and robust technique to pave the road for scaling up the required large plastic zones for dislocation engineering in ceramics.

**KEYWORDS**

cyclic loading, dislocations in ceramics, room-temperature plasticity, scratching

## 1 | INTRODUCTION

Recent promising proofs-of-concept for using *dislocations in ceramics* to harvest versatile mechanical and functional properties have encouraged increasing research endeavors in this rising field. Mechanically, engineering dislocations into ceramics increases the plastic deformability,<sup>1</sup> damage tolerance, and fracture toughness.<sup>2,3</sup> Functionally, dislocations have been demonstrated to tune superconductivity,<sup>4</sup> thermal conductivity,<sup>5</sup> and ferroelectric properties<sup>6</sup> in recent years. Successful engineering and controlling of dislocations in ceramics is anticipated to catalyze the revolution of *dislocation technology* in ceramics.<sup>7</sup> Regardless of these exciting new findings, it remains a great challenge to

engineer dislocation structures, particularly at room temperature, into normally brittle ceramics that are prone to cracking.

High-temperature deformation, being either uniaxial bulk compression<sup>8</sup> or local indentation technique,<sup>9</sup> very often requires a temperature above, for example,  $800^\circ\text{C}$  to provide thermal activation for sufficient dislocation mobility in ceramics. This may help to avoid crack formation as in the usual case at room temperature. However, it would incur much more energy consumption and a much longer time duration due to the heating process. On the other hand, room-temperature deformation could minimize energy consumption, but it also casts a higher risk of fracturing the sample with experiments performed

This is an open access article under the terms of the [Creative Commons Attribution](https://creativecommons.org/licenses/by/4.0/) License, which permits use, distribution and reproduction in any medium, provided the original work is properly cited.

© 2023 The Authors. *Journal of the American Ceramic Society* published by Wiley Periodicals LLC on behalf of American Ceramic Society.

under unfavorable mechanical loading conditions. So far, the majority of works for room-temperature plastic deformation while suppressing crack formation in ceramics were performed at nano-/microscale using nanoindentation tests<sup>10,11</sup> or micropillar compression.<sup>12</sup> The former benefits from the extremely localized high shear stress (beneficial for dislocation gliding) and high hydrostatic compressive stress (beneficial for crack closure) underneath the indenter, while the latter usually has a large free surface area and fewer preexisting defects in the micropillars that avoid local dislocation pile-up to induce cracks. However, these nano-/microscale approaches greatly limit the size of the plastic zone, although these methods have their merits in establishing proofs-of-concept at smaller scales.<sup>13</sup>

In fact, quite some single-crystal ceramic materials can be plastically deformed at room temperature in bulk compression.<sup>14–19</sup> Yet, these approaches usually produce plastic zones that contain only narrow slip bands (e.g., several or tens of micrometers in width<sup>20</sup>) confined to discrete regions in bulk crystals. This not only limits the available dislocation-rich region for further testing but also leads to inefficient use of the entire crystals, which usually are very expensive.

To address this challenge of scaling up the plastic deformation in ceramics to produce large and continuous plastic zones at room temperature without fracture, we propose here a simple but powerful approach to cyclically scratch the sample surface to achieve a plastic zone up to mm or cm range, with dislocation densities up to  $\sim 10^{13}/\text{m}^2$ . This method is simple, fast, and cost-effective, and we demonstrate its general applicability here on single-crystal  $\text{SrTiO}_3$ ,  $\text{MgO}$ ,  $\text{ZnS}$ , and  $\text{CaF}_2$ . Our method is expected to facilitate the mass production of dislocations in ceramics for harvesting both mechanical and functional properties.

## 2 | EXPERIMENTAL PROCEDURE

Un-doped, single-crystal (001)  $\text{SrTiO}_3$  (Alineason Materials Technology GmbH, Frankfurt am Main, Germany) was used for the scratching tests on a universal hardness testing machine (Karl-Frank GmbH, Weinheim-Birkenau, Germany) and mounted with a Brinell indenter and a controllable moving single-axis stage (PI Line M-6832V4, Physik Instrumente GmbH & Co. KG, Karlsruhe, Germany). The samples have a minimum thickness of 1 mm, with the side lengths varying from  $\sim 5$  up to  $\sim 10$  mm. A hardened stainless-steel spherical indenter (Habu Hauck Prüftechnik GmbH, Hochdorf-Assenheim, Germany) with a tip diameter of 2.5 mm was used for the cyclic scratching. During the scratching tests, the indenter was first placed

in contact with the sample mounted on the moving stage, which is controlled by a computer program for setting the speed of the stage (0.5 mm/s). For validating the method on other materials, we further tested (001)  $\text{MgO}$ , (001)  $\text{ZnS}$ , and (111)  $\text{CaF}_2$  surfaces. A load of 1 kg is chosen for all the samples (except for 0.8 kg on  $\text{ZnS}$  tested in darkness<sup>17</sup> to avoid cracking). Silicon oil was used as a lubricant to reduce wear of the tip as well as crack formation after a high number of scratching cycles.

The surface slip traces after deformation were visualized using optical microscopy (Zeiss Axio Imager2, Carl Zeiss AG, Oberkochen, Germany) in the circularly polarized light–differential interference contrast mode (C-DIC), which enhances the surface features with high resolution and contrast. The obtained images were consistently post-processed and presented as grey-scale images. Dark-field mode imaging was used to exclude visible crack formation underneath the surface. The dislocation density and etch pit patterns (recipe for chemical etching of  $\text{SrTiO}_3$  is provided elsewhere<sup>21</sup>) in the plastic zone were characterized with a laser confocal microscope (LEXT OLS4000, Olympus IMS, Waltham, USA) for better identification of surface features (e.g., dislocation etch pits) after surface etching. Transmission electron microscope (TEM) specimens were prepared from a reference and  $20\times$  scratch track on  $\text{SrTiO}_3$  single-crystal using a dual-beam focused ion beam instrument (Helios Nanolab 600i, FEI, Hillsboro, USA). Bright-field TEM imaging was conducted in a transmission electron microscope (FEI Talos F200X G2, Thermo Fisher Scientific, USA) at an operating voltage of 200 kV.

## 3 | RESULTS AND ANALYSES

We first demonstrate the scratch tracks on single-crystal (001)  $\text{SrTiO}_3$ . The length of the scratch tracks was set to be 4 mm in the current work (Figure 1A). However, we note that the maximum length of the plastic zone is tunable depending on the sample size. The slip traces are evidenced in Figure 1B,C for different scratching cycles ( $1\times$  and  $10\times$  for 1 cycle and 10 cycles, respectively), while no macroscale cracks were visible (Figure S1 in Supplementary Materials, Section 1.). Here, we define one cycle ( $1\times$ ) by simply one transverse sliding of the indenter on the sample surface in one direction (indicated by the yellow arrow in Figure 1B,C).

Inside the scratch tracks, we observe numerous horizontal and vertical slip traces, which correspond to intersections of  $\{110\}$  slip planes with the (001) surface being scratched. When indenting on the (001) surface of  $\text{SrTiO}_3$ , four equivalent slip planes ( $\bar{1}01$ ,  $101$ ,  $0\bar{1}1$ , and  $011$ ) with a  $45^\circ$  inclination to the indented surface can be

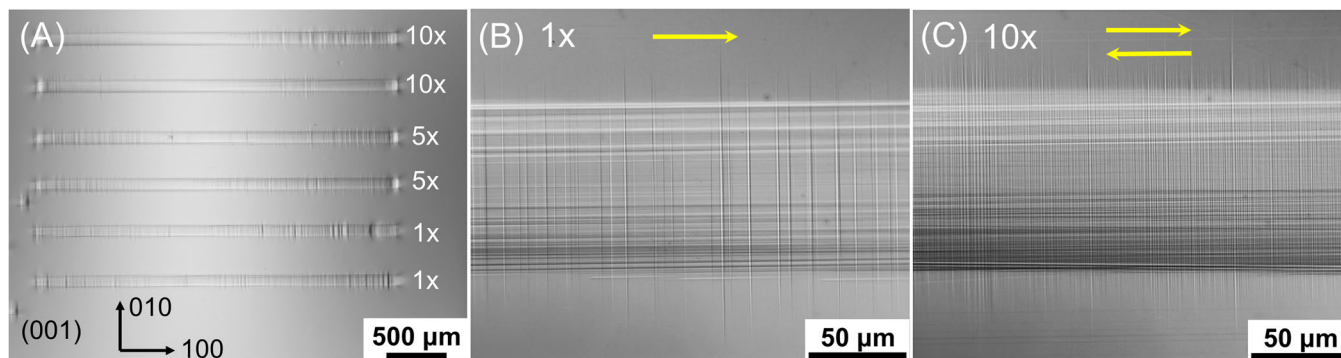


**FIGURE 1** Optical microscope images highlighting the plastic scratch tracks generated at room temperature with different scratching cycles on single-crystal (001) SrTiO<sub>3</sub>: (A) an overview of the scratch tracks; (B) representative scratch track with 1× scratching; (C) representative scratch track with 10× (10 cycles) scratching.

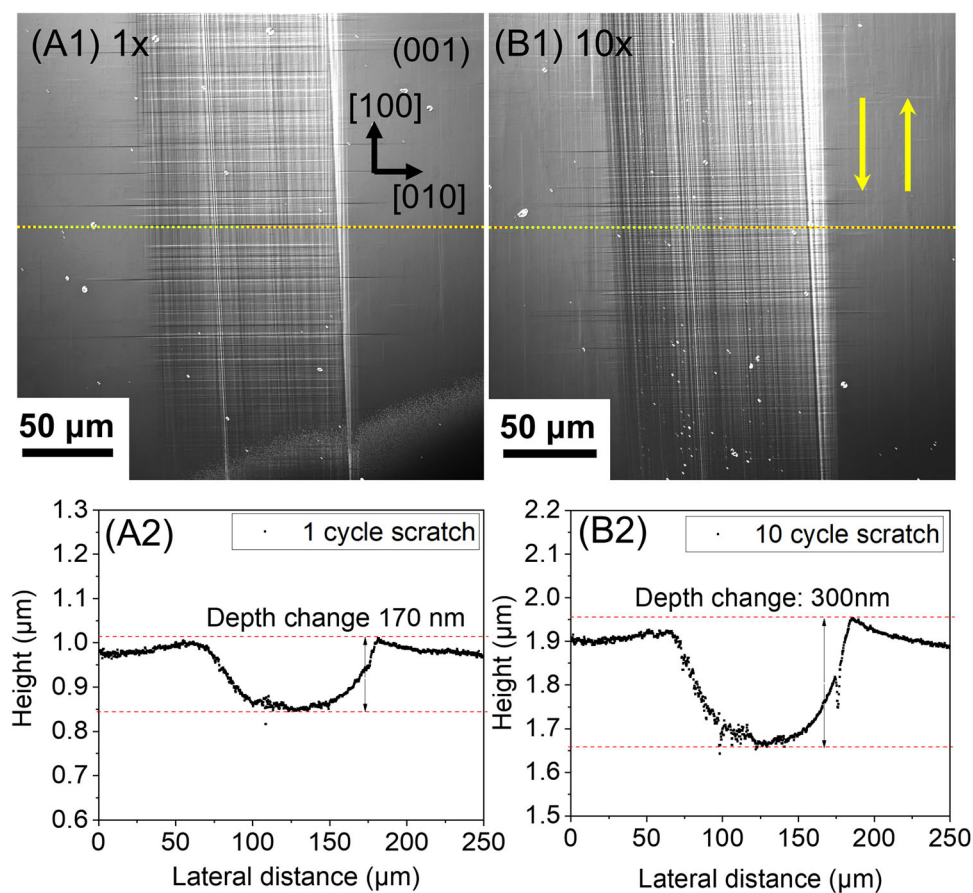


**FIGURE 2** Confocal laser microscope images featuring the surface topography of representative scratch tracks, with the cross-sectional profile extracted: (A1-2) 1× scratch; (B1-2) 10× scratch. The yellow arrows in sub-figure B1 indicate the (repeated) scratching directions.

activated.<sup>21,22</sup> A clear increase in the number of slip traces from 1× (Figure 1B) to 10× (Figure 1C) is evident, indicating an increase in the dislocation density, as will be confirmed later by the chemical etching method. A slight widening of the scratch track is also observed.

Consider that the slip systems of  $\{110\} \langle 110 \rangle$  are fixed in SrTiO<sub>3</sub> at room temperature,<sup>21,22</sup> it is therefore expected

that the scratch-induced slip traces would display a different surface pattern with respect to the scratch directions. This is clearly demonstrated in Figure S2 (Supplementary Materials, Section 2.), with a preset angle of 15 and 45° between the scratch direction and the  $\langle 100 \rangle$  direction.

Note that in Figure 1 the scratch tracks seem to be rather deep, which is due to the C-DIC imaging mode in the

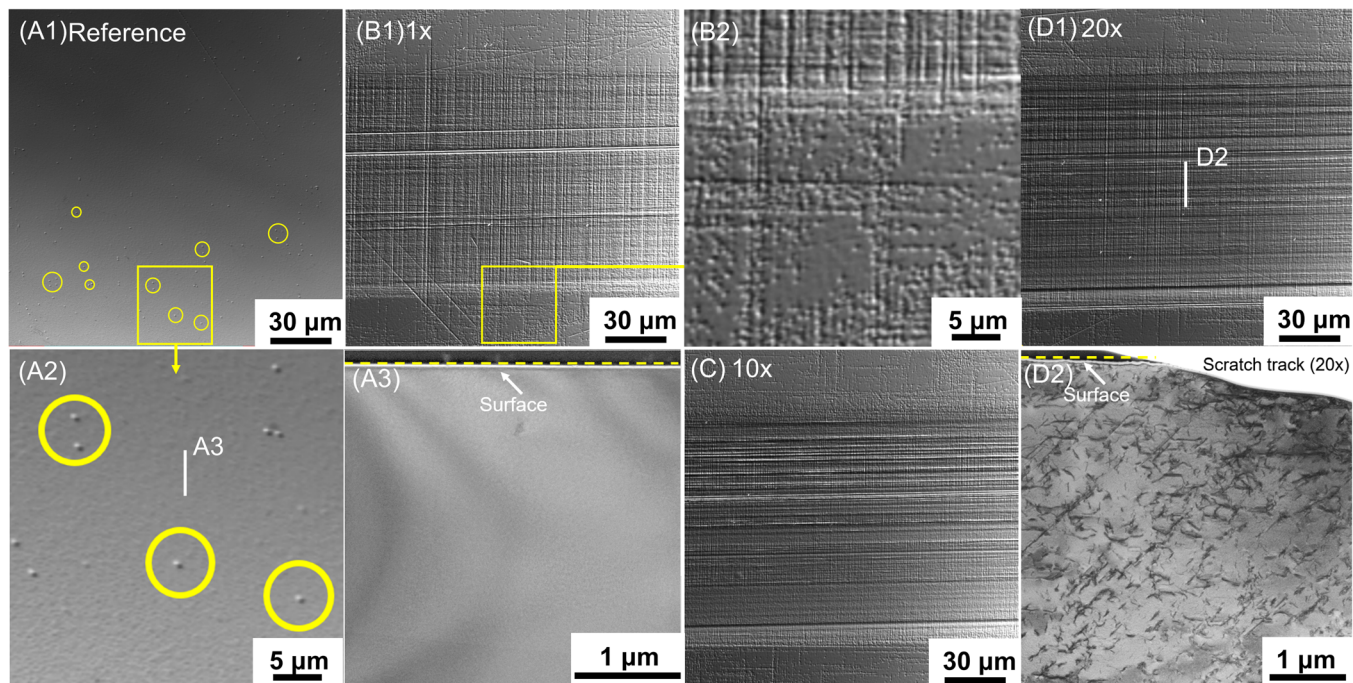


**FIGURE 3** Visualization of dislocations and slip traces in the samples under different conditions: (A1,2) a few dislocation etch pits are revealed by the chemical etching method in the reference region without scratching; (A3) bright-field transmission electron microscope (TEM) image showing almost dislocation-free region underneath the surface; (B1,2) dislocation etch pits for 1× scratching inside and adjacent to the scratch track; (C) 10× scratch track after chemical etching; (D1) 20× scratch track after chemical etching; (D2) bright-field TEM image of the abundant newly generated dislocations (indicated by the dark lines) underneath the surface after 20× scratching. The zoomed-in regions in (A2) and (B2) highlight the tiny dots which correspond to the dislocation etch pits, and the white vertical lines in (A2) and (D1) indicate the positions for lift-out of the TEM lamella.

optical microscopy enhancing the surface contrast on purpose. To quantify the change in depth across the scratch tracks with various numbers of scratching, we employed a confocal laser microscope. Figure 2 features the depth of the scratch track being  $\sim 170$  nm after 1×, and only increased up to  $\sim 300$  nm after 10× scratching. Considering the scratch track has a width of  $\sim 125$   $\mu\text{m}$ , the apparent surface undulation across the scratch track can be considered negligible (which also makes it rather challenging to detect such wide scratch tracks in a scanning electron microscope).

Correspondingly, the images in Figure 3 demonstrate changes in dislocation densities in the center region of the plastic scratch tracks after 1×, 10×, and 20× scratching. The reference sample has a dislocation density of  $\sim 10^{10}$   $\text{m}^{-2}$  (Figure 3A). After 1× scratching, the dislocation density increased to  $\sim 10^{12}$   $\text{m}^{-2}$  (Figure 3B) but with a rather discrete and scattered distribution of the etch pits in a horizontal and vertical arrangement (as in the case of the slip trace pattern in Figure 1B). Further increase of the number of cycles to 10× (Figure 3C) leads to an almost uniform and dense distribution of the dislocation etch pits, which is similar to that for 20× (Figure 3D1). Furthermore, the bright-field TEM image (Figure 3D2)

provides further direct visualization of abundant newly generated dislocations underneath the scratch track. The saturated dislocation density is found to be of the order of  $\sim 10^{13}$   $\text{m}^{-2}$ , which is similar to the approach of cyclic indentation loading.<sup>22</sup>

The increase of dislocation density as a function of increased scratching cycle number is attributed to dislocation multiplication mechanism, akin to effects in the large spherical ball indentation.<sup>22</sup> The multiplication of the dislocations inside one slip plane is most likely dominated by Frank-Read sources,<sup>23,24</sup> while the formation of a much higher number of slip traces at a higher number of scratching cycles may be governed by cross slip,<sup>22</sup> similar to the case of LiF.<sup>14</sup> The major difference here is the stress distribution under ball indentation and ball scratching, which will be investigated in greater detail in future works.

The general applicability of this scratching approach is further demonstrated on other ceramic materials at room temperature. In Figure 4, we showcase the continuous plastic scratch tracks on single-crystal (001) MgO, (001) ZnS, and (111) CaF<sub>2</sub>. Together with the cyclic loading approach, by overlapping the scratch tracks, a much larger area of plastic zone can be generated (Figure S3 and Figure S4 in Supplementary Materials, Section 3).

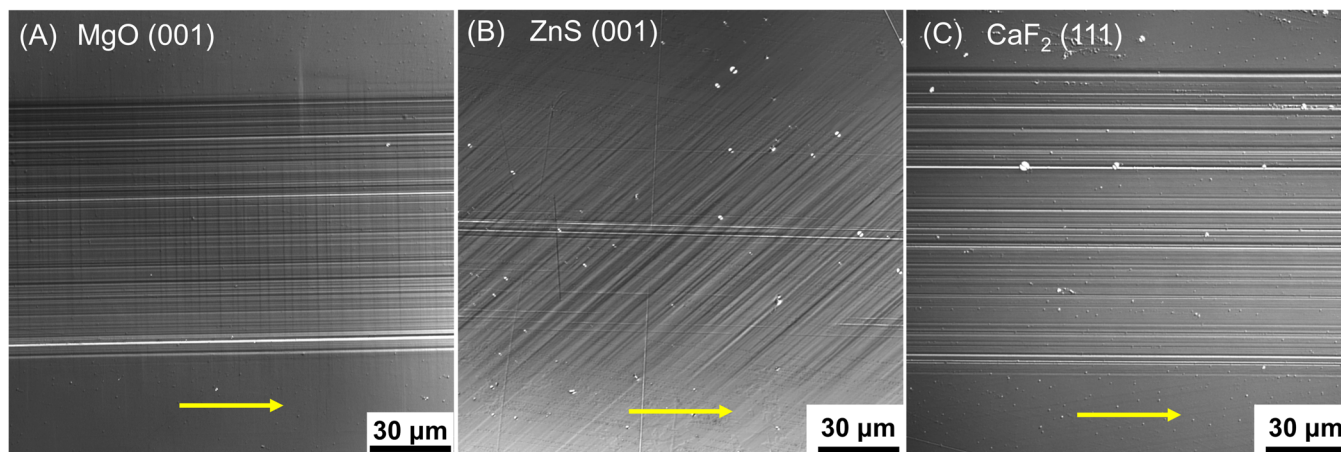


**FIGURE 4** Extension of the method to other materials: (A) MgO (001), (B) ZnS (001), and (C) CaF<sub>2</sub> (111) at room temperature, with 1× scratching for all three samples. All samples reveal clear slip traces inside the scratch tracks. The yellow arrows indicate the sliding direction.

Detailed analyses of the dislocation density, dislocation meso-structure, and the dislocation-based functional and mechanical properties will be pursued in follow-up works.

#### 4 | CONCLUSION

We demonstrate a simple but powerful experimental method to efficiently increase the dislocation-mediated plastic zone in various ceramics at room temperature. By using a large Brinell indenter (2.5 mm in diameter) for cyclic scratching on the surface of single-crystal SrTiO<sub>3</sub>, we succeeded in engineering continuous plastic zones with arbitrary lengths depending on the sample size. After 10 cycles of repetitive scratching inside the same scratch track, a saturation of slip lines, as well as dislocation density inside the plastic zone, is identified, with the dislocation density above  $\sim 10^{13} \text{ m}^{-2}$ . This simple technique guarantees sufficiently large plastic volumes with high dislocation density for future assessment of dislocation-tuned functional and mechanical properties. The applicability of this experimental approach is further validated on single-crystal MgO, ZnS, and CaF<sub>2</sub>, all at room temperature. This experimental approach may hold great potential for various ceramics if it is further extended to high-temperature rolling.<sup>25</sup>

#### ACKNOWLEDGMENTS

X. F. acknowledges the Athene Young Investigator Program at TU Darmstadt for supporting the research. O. P. acknowledges the funding by the Deutsche Forschungsgemeinschaft (DFG, No. 414179371). The authors thank Prof. J. Rödel for commenting on the original manuscript and Prof. K. Durst at TU Darmstadt for the access to the laser microscope. They also thank C. Okafor for

providing the cross-sectional view of the dislocation and plastic zone evolution after cyclic loading in the Supplementary Materials.

Open access funding enabled and organized by Projekt DEAL.

#### ORCID

Xufei Fang  <https://orcid.org/0000-0002-3887-0111>

#### REFERENCES

- Li J, Wang H, Zhang X. Nanoscale stacking fault-assisted room temperature plasticity in flash-sintered TiO<sub>2</sub>. *Sci Adv.* 2019;5:eaaw5519.
- Porz L, Klomp AJ, Fang X, Li N, Yildirim C, Detlefs C, et al. Dislocation-toughened ceramics. *Mater Horiz.* 2021;8:1528–37.
- Salem MN, Ding K, Rödel J, Fang X. Thermally enhanced dislocation density improves both hardness and fracture toughness in single-crystal SrTiO<sub>3</sub>. *J Am Ceram Soc.* 2023;106:1344–55.
- Hameed S, Pelc D, Anderson ZW, Klein A, Spieker RJ, Yue L, et al. Enhanced superconductivity and ferroelectric quantum criticality in plastically deformed strontium titanate. *Nat Mater.* 2022;21:54–61.
- Khafizov M, Pakarinen J, He L, Hurley DH. Impact of irradiation induced dislocation loops on thermal conductivity in ceramics. *J Am Ceram Soc.* 2019;102(12):7533–42.
- Höfling M, Zhou X, Riemer LM, Bruder E, Liu B, Zhou L, et al. Control of polarization in bulk ferroelectrics by mechanical dislocation imprint. *Science.* 2021;372:961–64.
- Ikuhara Y. Nanowire design by dislocation technology. *Prog Mater Sci.* 2009;54(6):770–91.
- Nakamura A, Lagerlöf KPD, Matsunaga K, Tohma J, Yamamoto T, Ikuhara Y, et al. Control of dislocation configuration in sapphire. *Acta Mater.* 2005;53(2):455–62.
- Holmes D, Heuer AH, Pirouz P. Dislocation structures around Vickers indents in 9.4 mol% Y<sub>2</sub>O<sub>3</sub>-stabilized cubic ZrO<sub>2</sub> single crystals. *Philos Mag A.* 1993;67(2):325–42.

10. Fang X, Bishara H, Ding K, Tsybenko H, Porz L, Höfling M, et al. Nanoindentation pop-in in oxides at room temperature: dislocation activation or crack formation? *J Am Ceram Soc.* 2021;104:4728–41.
11. Nakamura R, Masuda H, Yoshida H. Nanoindentation responses near single grain boundaries in oxide ceramics. *J Am Ceram Soc.* 2022;106(3):2061–72.
12. Korte-Kerzel S. Microcompression of brittle and anisotropic crystals: recent advances and current challenges in studying plasticity in hard materials. *MRS Commun.* 2017;7(2):109–20.
13. Bishara H, Tsybenko H, Nandy S, Muhammad QK, Frömling T, Fang X, et al. Dislocation-enhanced electrical conductivity in rutile TiO<sub>2</sub> accessed by room-temperature nanoindentation. *Scr Mater.* 2022;212:114543.
14. Johnston WG, Gilman JJ. Dislocation multiplication in lithium fluoride crystals. *J Appl Phys.* 1960;31(4):632–43.
15. Argon AS, Orowan E. Plastic deformation in MgO single crystals. *Philos Mag.* 1964;9(102):1003–21.
16. Brunner D, Taeri-Baghdadrani S, Sigle W, Rühle M. Surprising results of a study on the plasticity in strontium titanate. *J Am Ceram Soc.* 2001;84(5):1161–3.
17. Oshima Y, Nakamura A, Matsunaga K. Extraordinary plasticity of an inorganic semiconductor in darkness. *Science.* 2018;360:772–4.
18. Mark AF, Castillo-Rodriguez M, Sigle W. Unexpected plasticity of potassium niobate during compression between room temperature and 900°C. *J Eur Ceram Soc.* 2016;36(11):2781–93.
19. Munoz A, Rodriguez AD, Castaing J. Plastic deformation of CaF<sub>2</sub> single crystals. *Radiat Eff Defects Solids.* 2006;137(1-4):213–5.
20. Kissel M, Porz L, Frömling T, Nakamura A, Rödel J, Alexe M. Enhanced photoconductivity at dislocations in SrTiO<sub>3</sub>. *Adv Mater.* 2022;34:2203032.
21. Javaid F, Stukowski A, Durst K. 3D dislocation structure evolution in strontium titanate: spherical indentation experiments and MD simulations. *J Am Ceram Soc.* 2017;100(3):1134–45.
22. Okafor C, Ding K, Zhou X, Durst K, Rödel J, Fang X, et al. Mechanical tailoring of dislocation densities in SrTiO<sub>3</sub> at room temperature. *J Am Ceram Soc.* 2022;105:2399–402.
23. Caillard D, Martin JL. Thermally activated mechanisms in crystal plasticity. Oxford, UK: Pergamon; 2003.
24. Hull D, Bacon DJ. Introduction to dislocations. Oxford, UK: Butterworth-Heinemann, Elsevier; 2011.
25. Li Y, Tan C. Enhancing the mechanical properties of ceramics by high temperature rolling: a first demonstration using alumina. *J Am Ceram Soc.* 2022;106(3):1644–6. <https://doi.org/10.1111/jace.18895>

## SUPPORTING INFORMATION

Additional supporting information can be found online in the Supporting Information section at the end of this article.

**How to cite this article:** Fang X, Preuß O, Breckner P, Zhang J, Lu W. Engineering dislocation-rich plastic zones in ceramics via room-temperature scratching. *J Am Ceram Soc.* 2023;106:4540–4545. <https://doi.org/10.1111/jace.19140>